Sorption of selenium(IV) and selenium(VI) to mackinawite (FeS): Effect of contact time, extent of removal, sorption envelopes

Dong Suk Han [a,*], Bill Batchelor [b], Ahmed Abdel-Wahab [a]

[a] Chemical Engineering, Texas A&M University at Qatar, Education City, PO Box 23874, Doha, Qatar
[b] Zachry Department of Civil Engineering, Texas A&M University, College Station, TX 77843-3136, United States

ABSTRACT

Higher concentrations (127, 253 μM) of Se(IV) at pH 8 were completely removed by 0.5 g/L FeS within 120 min. Removal of Se(VI) by FeS at pH 8 was less extensive than removal of Se(IV). Only 10% of the Se(VI) was removed by 1 g/L FeS within 1 h. Removal patterns for Se by FeS depend on pH. Removal patterns of Se at pH 7 and pH 8 were best described by BET models for Se(IV) and Freundlich models for Se(VI), while removal patterns of both at pH 9 and 10 were best described by Langmuir models. Sulfate at 1 and 10 mM had negligible effect on removal of Se(IV) by FeS, while sulfate had little effect on removal of Se(VI) by FeS, but there was some indication that sulfate promoted removal of Se(VI) at intermediate concentrations. The test for the effect of pH on sorption of Se(IV) by FeS showed nearly complete removal at all but the high initial pH. When pH was raised back to initial value, greater removals were observed than initially. Mixtures of Se(VI) and FeS showed moderate removal at low pH, a minimum removal near pH 6 and nearly complete removal at high pH. Very high stability was observed with negligible release as pH decreased.

© 2010 Elsevier B.V. All rights reserved.

1. Introduction

Selenium is known to be an essential nutrient for animals and humans, although it is not essential for plant growth [1]. It can be toxic to animals that consume plants with sufficiently high levels [1]. For instance, leaching of Se-rich soils by agricultural drainage in the San Joaquin valley was found to result in extremely harmful levels, with concentrations in drainage water approaching 140–1400 μg/L. These concentrations are high enough to cause carcinogenic and teratogenic effects [2]. In addition, chronic exposure to low levels of Se can cause developmental abnormalities and reproductive disorders. The difference in Se concentrations that cause nutrient deficiency and toxicity is smaller than that noted for other USEPA priority or non-priority pollutant [3,4].

Selenium is an analogue of sulfur, so they are similar in aquatic chemistry [5]. The primary selenium species in oxidized water are selenate ($Se^{VI}O_4^{2-}$), selenite ($Se^{IV}O_3^{2-}$) and their protonated forms. The pK_a values for selenic acid (H_2SeO_4) are <1 and 1.7, and those for selenious acid (H_2SeO_3) are 2.75 and 8.5 [5]. Therefore, at pH 7, the primary species will be SeO_4^{2-} and $HSeO_3^{-}$. Under more reducing conditions, zero-valent selenium and hydrogen selenide (H_2Se) can be found. The pK_a values for hydrogen selenide (H_2Se) are 3.89 and 15, so HSe^- will be the primary Se species as $-II$ observed in the pH range of most natural waters. Se(IV) and Se(VI) are the most mobile forms of selenium, while Se(0) and Se($-II$) are relatively immobile because of the low solubility of their solid phases. Se(IV) is more toxic than other forms and that is why Se(IV) removal is extensively studied [6].

A variety of treatment technologies, including reverse osmosis, ion exchange, coagulation, adsorption, and biological treatment, have been applied in order to remove selenium from water [7–9]. Among them, adsorption using Fe-, Mn-, or Al-oxyhydroxides has been extensively studied because adsorption of aqueous Se species onto such mineral surfaces plays an important role in determining the mobility and bioavailability of selenium [10–12]. Although these treatment methods can lower both Se(IV) and Se(VI) to below 5 μg/L, they are not suitable for Se(VI) in wastewaters originating at coal-fired power plants or mining activities containing high concentration of sulfate because chemical property of sulfate is quite similar to that of Se(VI), resulting in significant decrease of removal of Se(VI) by competitive adsorption [13,14]. Very little information is now available about selenium removal in sulfate-rich environments. Furthermore, removal of selenium by adsorption onto iron oxyhydroxides will have a possibility for not producing stable residuals under the anoxic conditions found in landfills due to reductive dissolution of ferric to ferrous iron, possibly resulting in release of Se to environment.

Reduction of Se(IV) and Se(VI) to Se(0) or Se($-II$) is required to form solid phases with low solubility and therefore, low mobility

* Corresponding author. Tel.: +974 4423 0519; fax: +974 4423 0065.
E-mail address: dong_suk.han@qatar.tamu.edu (D.S. Han).

in the environment. Zero-valent selenium and HSe$^-$ in subsurface environments can form less soluble solid phases such as metal sulfide ores that include Fe, Cu, and Pb [15–17]. Recent studies demonstrate that selenite can be reduced to insoluble Se(0) after contact with Fe(II)-bearing minerals such as mackinawite and magnetite with the final product being two iron selenides (Fe$_7$Se$_8$ and FeSe) [18].

Previous research has demonstrated that mackinawite (FeS) can be a good reactant/adsorbent to remove selenium from water [19]. This study aims to provide fundamental information on the behavior of Se with adsorbent/reactant (FeS) as well as the basis for development of treating processes for ash and scrubber pond waters at coal-fired power plants that will be effective in removing Se and will produce residuals with low solubility. However, more detailed studies are needed to evaluate the capability of mackinawite for removal of Se(IV,VI) under a range of various solution conditions that are suitable for ash and scrubber pond waters. To do so, this study aims to investigate the effect of time on Se(IV,VI) removal by mackinawite, to measure the effect of pH on the extent of removal with and without the presence of a competing ion (sulfate), and to evaluate the sorption envelopes of Se(IV,VI) by mackinawite when pH changes. To better understand chemical changes that affect sorption envelope of Se(IV,VI) by mackinawite, X-ray photoelectron spectroscopy will be used to characterize chemical species on the surface of the solid-phases.

2. Materials and methods

2.1. Materials

All of the chemicals used in this study were analytical grade or better and all solutions were prepared using deionized/deoxygenated (DI/DO) water (>18 MΩ^{-1} resistivity). The water was deoxygenated by purging with high purity nitrogen for more than 2 h and contacting it with the atmosphere of an anaerobic chamber for at least one day. Sodium selenite (Na$_2$SeO$_3$) and sodium selenate (Na$_2$SeO$_4$) were purchased from Sigma–Aldrich. Mackinawite (FeS) was synthesized according to the method described in a previous study [24] that followed the recipe of the Hayes research group [20,21]. In short, 0.1 M Na$_2$S and 0.1 M FeCl$_2$ were initially mixed with equivalent volume ratio and then they were aged for 3 days. According to previous result, the synthesized FeS was identified to amorphous mackinawite [19]. The surface area of synthesized FeS was reported in literatures, ranging from 0.05 to 424 m^2/g [22,23]. This considerable difference may be caused by both aggregations of FeS particles during sample preparation and measurement methods. The prepared suspension of FeS was used to removal selenium as a reactant/adsorbent. Se(IV) and Se(VI) stock solutions (1000 mg/L) were prepared by dissolving Na$_2$SeO$_3$ and Na$_2$SeO$_4$ in DI/DO water. All sorption experiments were performed in an anaerobic chamber (95% N$_2$/5% H$_2$) with palladium catalyst that maintained O$_2$ concentrations near zero.

2.2. Sorption experiments

Initial time-dependent sorption experiments were conducted at pH 8 to evaluate removal of Se(IV) and Se(VI) by suspensions of 1 g/L FeS with different initial concentrations of selenium (6.3, 12.7, 38, 127, 253 μM Se(IV); 12.7, 38, 127 μM Se(VI)). Reactions were initiated by adding Se(IV) or Se(VI) stock solution to 20-mL suspension of FeS in 25-mL reaction vessels and then mixing by reciprocal rotator. A 10-mL aliquot was sampled from the suspensions containing Se(IV) at reaction times of 0.5, 1, 2, 3, 6, 9, 18, 30, 43.7 h. Similar samples were taken from the suspensions containing Se(VI) after reaction times of 1, 3, 7, 10, 19, 25, 32, 44, 49,

57, 68, 100 h. The samples were immediately filtered using 0.02-μm anodisc membrane filters and the filtrates were stored in an anaerobic chamber until measurement using hydride generation atomic absorption spectroscopy (HGAAS). Experiments to evaluate removal of Se(IV) and Se(VI) by suspensions of FeS were conducted in a similar way to those previously conducted to evaluate removal of Se(IV) by suspensions of pyrite [24]. The effect of pH (7, 8, 9, 10) on removal of Se(IV) and Se(VI) by FeS was evaluated in a series of batch experiments. The initial aqueous-phase concentrations of Se(IV) ranged from 63.3 to 2508 μM and the initial concentrations of Se(VI) ranged from 6.5 to 1395 μM. A constant concentration of FeS of 1.0 g/L was used and the mineral form of FeS was mackinawite. The pH of the suspensions was adjusted by 0.5 M HCl or 0.5 M NaOH. Samples were taken after 24 h of reaction and analyzed for Se(IV) or Se(VI). Experiments to determine the effect of sulfate on selenium removal were conducted similarly at pH 8 and at two sulfate concentrations (1 and 10 mM).

2.3. Adsorption envelope of selenium

To investigate the effect of pH on sorption of Se(IV) and Se(VI) by FeS, the experimental method used by Bostick and Fendorf was modified [25]. This method measures removal of selenium as a function of pH, which is adjusted by addition of 1 or 2 M of HCl or NaOH. The experiments were initiated by adjusting pH near pH 10 (for Se(IV)) or pH 4.0 (for Se(VI)) and then selenium was added to obtain a concentration of 16.5 μM. The starting pH was specified as the value where removal of selenium was lowest, as indicated by preliminary experiments or reports in the literature, so that the reverse titration of pH at maximum sorption level can allow us to evaluate sorption envelope as well as sorption hysteresis. An initial sample was taken after 30 min and then pH was adjusted to desired values. Samples of 10 mL were taken after 30 min reaction at each pH and they were filtered with 0.02-μm pore sized anodisc membrane filters. Herein, samples will be identified with the following nomenclature to simplify the discussion. For Se(IV)-contacted mackinawite, the initial sample at pH 10 will be named the "pH 10$_{(i)}$" sample and the sample at pH 4 after acid titration will be named the "pH 4$_{(a.a.t)}$" sample. Another stability test was conducted for the Se(VI) in a similar way, but the initial pH was pH 4. Thus the initial sample at pH 4 will be named the "pH 4$_{(i)}$" sample and the samples at the pH 6 and 10 after base titration will be named the "pH 6$_{(a.b.t)}$" and "pH 10$_{(a.b.t)}$", respectively. The filtered samples were stored in an anaerobic chamber until selenium analysis by AAS in order to prevent changes in the redox states of selenium.

2.4. Spectroscopic analyses

XPS spectra were obtained using a KRATOS Axis Ultra Imaging X-ray photoelectron spectrometer with a monochromatized Al Kα (1253.6 eV) source. The detailed analysis procedure was described in a previous study [24]. Briefly, a filter disk containing solid samples were attached to a copper adhesive on a sample bar, which was then loaded to the sample treatment chamber (STC) that was evacuated to a pressure less than 5×10^{-7} Torr. Thereafter, the sample bar was transferred to the sample analysis chamber (SAC) where spectra were collected with a take-off angle close to 90°. The survey scans were obtained at a pass energy of 80 eV to determine chemical elements and the most characteristic spectra were recorded by the narrow scans with fixed pass energy of 20 or 40 eV to determine oxidation states and bonding type of element [26]. The charge effect was corrected using C 1s (E_b = 284.5 eV) to calibrate the binding energy scale. The XPS spectra were fitted using a program (XPSPEAK) that uses a Gaussian–Lorentzian function and background-subtraction corrections using a Shirley-type opti-
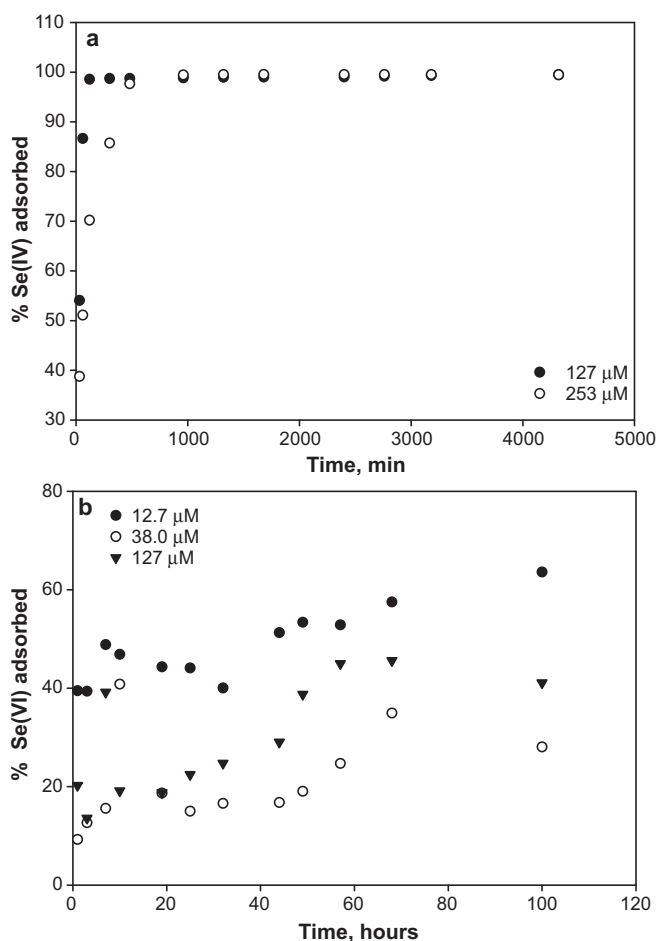
Fig. 1. Effect of time on concentrations of Se in presence of FeS at pH 8: (a) FeS = 0.5 g/L and Se(IV) = 127 and 253 μM; (b) FeS = 1 g/L and Se(VI) = 12.7, 38 and 127 μM.

mization. The surface species with various oxidation states were identified by comparison of their binding energies with literature values.

2.5. Measurement of selenium from aqueous concentrations

Selenium (IV,VI) was measured by a Perkin–Elmer atomic absorption spectrophotometer with a continuous flow, hydride generator. Selenite (SeO_3^{2-}) was measured without acid pretreatment, while selenate (SeO_4^{2-}) was first reduced to selenite by acid digestion (5 mL sample, 5 mL concentrated HCl in 40 mL borosilicate glass vial placed in boiling water bath for 10 min). The following parameters were used for these analyses: wavelength of 196.0 nm, band pass of 0.5 nm, lamp current of 75%, measurement number of 4, measurement time of 4 s, background correction is on, stabilization time of 30 s, baseline delay time of 40 s, carrier gas flow rate of 240 mL/min.

3. Results and discussion

3.1. Effect of contact time on Se sorption

Experiments for the effect of time on Se sorption were also conducted at higher Se(IV)/FeS ratios (Fig. 1a) because removal of Se(IV) by 1 g/L of FeS is so fast that Se(IV) can be completely removed within 30 min at all initial concentrations studied (6.3,

12.7, 38 μM) (Fig. S1). As a result of the higher ratios, Se(IV) was completely removed by 0.5 g/L of FeS within 120 min when the initial concentration was 127 μM, while complete removal of Se(IV) dosed at 253 μM occurs after 480 min. Also, no release of Se(IV) was observed at times longer than needed for complete removal. Meanwhile, the thick black FeS suspension turned red after contact with Se(IV). This color change was observed in all samples regardless of Se(IV)/FeS ratios, but the red color became more intense over time. However, it is difficult to clearly see the color differences in the suspensions because of plastic bottles. Furthermore, at higher Se(IV)/FeS ratio, the some solids were attached to the wall of the reactor vessel, that is likely due to change of physical/chemical properties of solid-phases. The results may support the formation of colloidal Se(0) particles through FeS-mediated Se(IV) reduction, followed by formation of surface precipitates such as FeSe or $FeSe_x$. Breynaert et al. [27] also observed red Se(0) particles on the surface of FeSe after FeS reacted with Se(IV) for 3 days. In contrast, Fig. 1b shows that more than 10% of Se(VI) is removed in the first hour, irrespective of initial concentration, followed by additional removal at a slow rate. The slower rate and lower extent of uptake of Se(VI) compared to that of Se(IV) may be due to a lower affinity of Se(VI) for the FeS surface. This would occur if the surface were negatively charged at pH 8, because Se(VI) would be present as an anion with two negative charges at pH 8, compared to Se(IV) which would be present mostly as an anion with one negative charge. The rapid and more favorable sorption of Se(IV) than Se(VI) by FeS is in a good agreement with most studies using metal oxides (goethite, hematite, alumina) [28–30], except that additional removal of Se(VI) occurred over time. Also, the amount removed is not strongly affected by increasing initial concentration at the lower values, but much higher amounts are removed at the highest initial concentration. However, no change in color was observed when Se(VI) was contacted with FeS, which indicates that Se(0) was not being formed.

3.2. Nonlinear removal patterns

3.2.1. Effect of pH

Fig. 2 shows the results of experiments describing removal of Se(IV) and Se(VI) by FeS at four different pH values. Models (BET, Langmuir, Freundlich) were fitted to the data and the values of model parameters were obtained by nonlinear regression (Table 1).

Results from experiments conducted at pH 7 and 8 are described best (lowest RFEP) by the BET isotherm model (Table 1) and results at other pH values are described best by the Langmuir isotherm that indicates the saturation of the surface sites. All isotherm equations are described in supporting information. Since Se(IV) removal at pH 7 and 8 is well described by the BET isotherm, it can be inferred that some multilayer sorption were occurring. For example, Se(IV) could be reduced to Se(−II) and precipitate as FeSe or $FeSe_x$ [16–18,27,31]. Similar sorption behaviors were also observed in other studies where As(III) removal by sulfide minerals (FeS, FeS_2, PbS, ZnS) was better described by a BET isotherm than a Langmuir isotherm, indicative of the development of polymeric cluster or surface precipitate via surface reaction [25,32,33]. Although the BET model was developed to describe a multilayer gas sorption, it could also represent a continuous accumulation of adsorbates on the solid surface that does not show the plateau region reaching a maximum level of sorption. The BET model is preferred for this use over a solid solution model because of its simplicity and ability to evaluate whether continuous adsorption (e.g., polymeric cluster, surface precipitates) occurs or not. The adsorption maximum on FeS at pH 7 exceeds 2500 μmol/g, which is higher than that of pyrite at pH 8 by four orders of magnitude, which indicates that FeS is much reactive with Se(IV) than pyrite [17].

Table 1
Summary of model parameters for Se(IV) removal by FeS.

Models	Solution pH			
	pH 7	pH 8	pH 9	pH 10
Langmuir				
q_{max} (μmol/g)	2206 ± 438	1377 ± 184	886 ± 56.6	787 ± 80
b (L/μmol)	0.00 ± 0.00	2.4 ± 3.3	3.67 ± 2.15	3.46 ± 3.94
SSR	1.6×10^4	4.7×10^5	3.9×10^4	7.7×10^4
RFEP	0.281	0.209	0.092	0.147
Freundlich				
k_f	319 ± 191	492 ± 136	436 ± 120	395 ± 215
n	3.65 ± 1.19	6.26 ± 1.62	9.43 ± 3.65	10.1 ± 8.2
SSR	2.2×10^5	7.8×10^4	6.0×10^4	1.9×10^5
RFEP	0.116	0.085	0.114	0.231
BET				
A	234 ± 193	$1.6 \times 10^4 \pm 1.0 \times 10^4$	$4.4 \times 10^4 \pm 3.1 \times 10^4$	$4.4 \times 10^4 \pm 8.2 \times 10^4$
q_{max}	1276 ± 67	1130 ± 62	790 ± 57	687 ± 107
SSR	9.9×10^4	4.9×10^9	4.9×10^4	1.7×10^5
RFEP	0.077	0.080	0.102	0.223

In contrast, Fig. 2b shows that the solid-phase concentrations of Se(VI) are below 140 μmol Se/g in all experiments, indicating that the sorption capacity of FeS for Se(VI) is much lower than for Se(IV). Maximum solid phase concentrations (q_{max}) for Se(VI) on FeS were observed to be in the range 20–140 μmol/g, which is comparable to that of Se(VI) on goethite, but is higher than that for hematite by a factor of 4.5 [34]. In addition, this range is similar to what was observed for removal of Se(IV) by pyrite [24], indicating that FeS was more reactive with Se than was pyrite. At pH 7 and 8, the solid-phase concentration increases rapidly at higher aqueous concentration, indicating that Se(VI) may be undergoing surface reactions. The Freundlich model fits this data best, while results of experiments conducted at pH 9 and pH 10 shows a pattern of removal that is better described by the Langmuir model (Table 2), which usually provides the best fit for data of Se(VI) sorption on iron oxides and hydroxides [34]. A pattern of removal that is more like that observed for experiments at lower pH might be observed at higher pH, if higher concentrations were investigated or more time were allowed for surface reactions to occur. For instance, extending contact time of Se(IV) with pyrite from 1 to 7 days resulted in an increase in maximum solid-phase concentration by a factor of 3 [17].

3.2.2. Effect of sulfate concentration

Fig. 3a shows that sulfate concentration of 1 and 10 mM had a negligible effect on removal of Se(IV) by FeS. The RFEP values show that the Langmuir model provides the better fit than does the Freundlich model (Table 3). The BET model was not fitted to

this data, because there was no indication in the data that followed a BET isotherm. Fig. 3b shows that there is little effect of sulfate on the amount of Se(VI) removed, although there is some indication that the higher level of sulfate resulted in increased Se(VI) removal when the concentrations of Se(VI) in solution were at intermediate levels. The enhanced removal of Se(VI) could be caused by association of another intermediate solid-phase product such as green rust (GR). GR is a Fe(II)–Fe(III) hydroxyl-salt that could be formed when reduction to Se(VI) by FeS produces Fe(III). GR with sulfate in its interlayer has been reported to be capable of reducing Se(VI) at basic pH. The Se(VI) is first reduced to Se(IV), which then forms bidentate binuclear and edge sharing complexes with Fe polyhedra that are slowly converted to Se(0) or Se(−II) [35]. However, this reaction pathway can occur rapidly when Se(VI) was exchanges with sulfate in the GR interlayer.

3.3. Adsorption envelopes of selenium

3.3.1. Liquid-phase analysis

Fig. 4 shows results of experiments for the effect of pH on sorption of Se(IV) and Se(VI) by FeS. For Se(IV), the pH was initially adjusted to near pH 10 and then lowered in a series of steps (Fig. 4a). The benefit of a continuous two-way pH titration is to easily evaluate the hysteresis of adsorption that indirectly implies the formation of the inner-sphere complexes, although there is a limitation to separate precipitation from sorption [25,32,36]. Nearly complete removal was observed for all pH values below about pH 9. As pH was raised, there was no release of Se(IV), even near pH

Table 2
Summary of model parameters for Se(VI) removal by FeS.

Models	Solution pH			
	pH 7	pH 8	pH 9	pH 10
Langmuir				
q_{max} (μmol/g)	$3.94 \times 10^4 \pm 1.29 \times 10^7$	$1.67 \times 10^5 \pm 2.17 \times 10^8$	31.2 ± 12.9	19.7 ± 7.95
b (L/μmol)	$2.16 \times 10^{-6} \pm 8.12 \times 10^{-4}$	$4.45 \times 10^{-7} \pm 5.89 \times 10^{-4}$	$7.4 \times 10^{-3} \pm 1.34 \times 10^{-2}$	$9.25 \times 10^{-3} \pm 1.8 \times 10^{-2}$
SSR	2.2×10^3	8.8×10^2	3.7×10^2	1.4×10^2
RFEP	0.40	0.26	0.33	0.32
Freundlich				
k_f	$2.3 \times 10^{-4} \pm 1.0 \times 10^{-3}$	$1.32 \times 10^{-3} \pm 4.4 \times 10^{-2}$	3.39 ± 7.24	3.01 ± 2.8
n	0.54 ± 0.19	0.63 ± 0.14	3.28 ± 3.55	3.85 ± 4.02
SSR	9.6×10^2	2.8×10^2	5.2×10^2	1.8×10^2
RFEP	0.26	0.15	0.39	0.36
BET				
A	15.8 ± 2.5	15.8 ± 2.4	28.3 ± 11.2	17.9 ± 6.86
q_{max}	55.2 ± 279	44.1 ± 175	$1.21 \times 10^2 \pm 237$	$1.56 \times 10^2 \pm 3.24 \times 10^2$
SSR	1.3×10^2	8.1×10^2	4.0×10^2	1.5×10^2
RFEP	0.30	0.25	0.34	0.33

Table 3
Summary of model parameters for Se(IV) removal as affected by sulfate (1 and 10 mM).

SO_4^{2-} (mM)	Langmuir				Freundlich			
	b (L/mol)	q_{max} (μmol/g)	SSR	RFEP	K_f (μmol$^{1-1/n}$ L$^{1/n}$/g)	n	SSR	RFEP
0	0.046 ± 0.058	1555 ± 198	2.8×10^5	0.16	588 ± 162	7.19 ± 2.16	5.1×10^5	0.17
1	0.024 ± 0.014	1541 ± 114	8.1×10^4	0.09	432 ± 157	5.68 ± 1.73	1.0×10^5	0.11
10	0.031 ± 0.026	1498 ± 173	1.8×10^5	0.13	495 ± 147	6.43 ± 1.87	9.0×10^5	0.19

10. Retention of Se(IV) after pH was raised to near pH 10 indicates that stronger bonds between Se(IV) and mackinawite were formed at the lower pH. For Se(VI) adsorption (Fig. 4b), pH was initially adjusted to near pH 4, raised in a series of steps, and then decreased in a series of steps to near pH 4. Removal of Se(VI) decreased as pH increased with a minimum near pH 6. Removals increased above pH 6 with nearly complete removal observed near pH 8 and above. No Se(VI) was released when pH was decreased. This indicates that strong bonds were formed by reaction between selenium and the FeS, possibly including redox reactions. Such reactions were observed in mixtures of Se(VI) and pyrite [24]. Both Se(IV) and Se(VI) are stable after contact with FeS when pH is optimal (i.e., pH 4–9 for Se(IV), pH 8–10 for Se(VI)) and sufficient time is allowed for surface reactions.

3.3.2. Solid-phase analysis

In order to elucidate the possible mechanisms of surface reactions between Se(IV) and FeS demonstrated by behavior shown in Fig. 4a, XPS analysis on the samples of FeS after contact at pH $10_{(i)}$ and pH $4_{(a.a.t)}$ were performed and the results are shown in Fig. 5a. When selenium sorbs to a surface that does not contain iron, the width and intensity of the selenium peak in the Se 3d spectra depends on the extent of sorption and the redox state of selenium [37]. However, when selenium sorbs to a surface that contains iron, the Se 3d spectra can be affected by interference caused by the Fe 3p spectra [2,31,38]. For the pH $4_{(a.a.t)}$ sample shown in Fig. 5a, the center of the Se 3d peak was located at a higher bonding energy than the pH $10_{(i)}$ sample, which is evidence that the pH $4_{(a.a.t)}$ sample was more reduced. Such a shift was shown in a previous study [24], where the Se 3d peak of Se(IV)-contacted mackinawite or pyrite was located at higher bonding energy after undergoing reduction. Thus, reduction of Se(IV) is more likely to have occurred on the pH $4_{(a.a.t)}$ sample than on the pH $10_{(i)}$ sample. It was reported that the mackinawite after contact with Se(IV) at pH 4.3 produced a tetragonal FeSe-like solid-phase that was identified by XAS (X-ray absorption spectroscopy), whereas at higher pH the nanoparticulate red Se(0) was produced [18]. Although XPS did
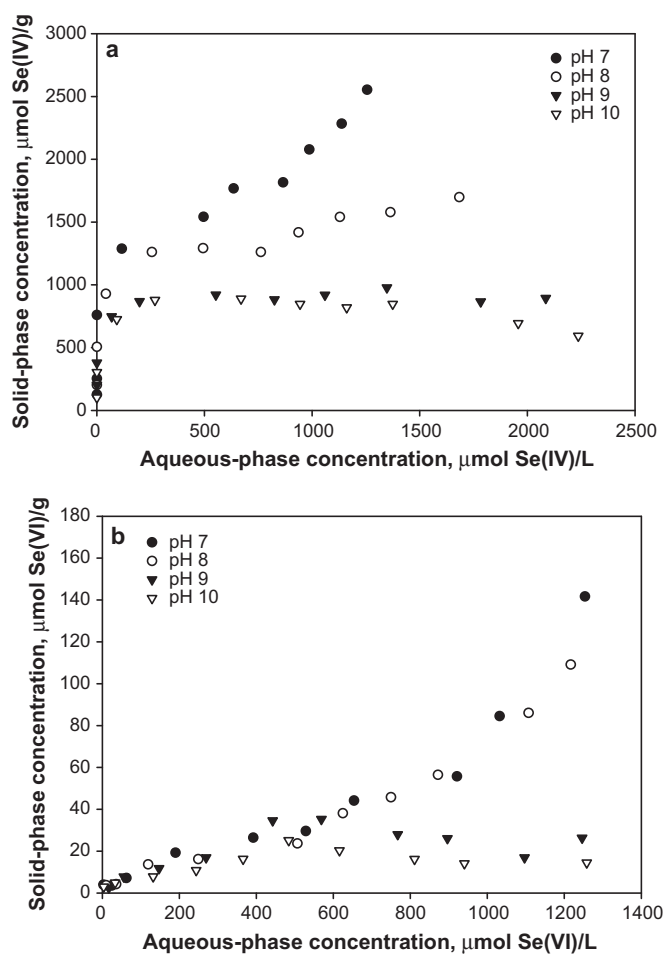

Fig. 2. Measured concentrations of (a) Se(IV) and (b) Se(VI) on FeS (symbols) as functions of concentration in water with BET model predictions (lines) at various pH: (a) 0.5 g/L FeS, 24 h of contact time; (b) 1.0 g/L FeS, 24 h of contact time.
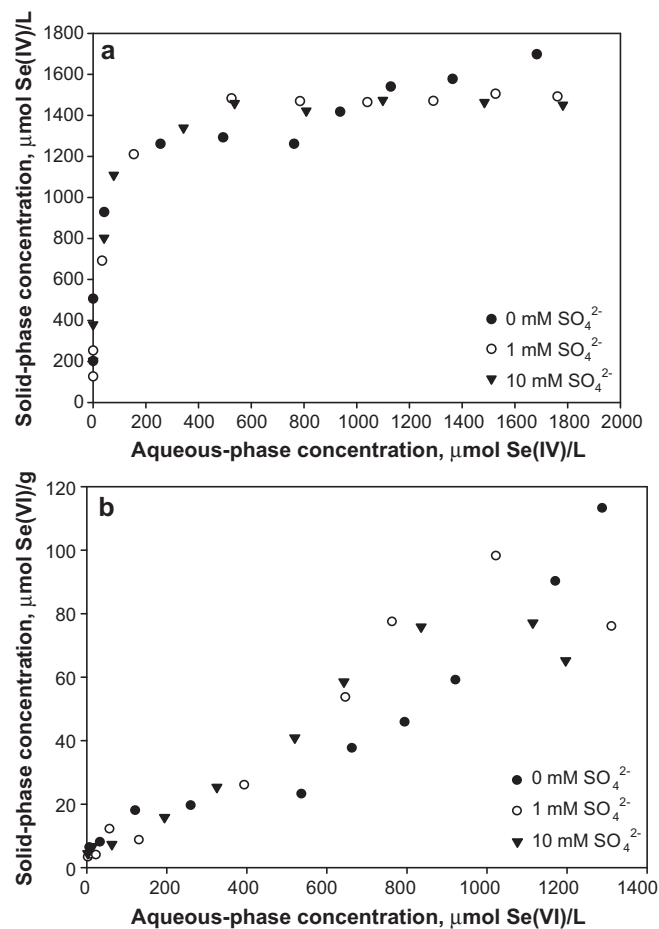
Fig. 3. Effect of sulfate on solid-phase concentration of (a) Se(IV) with prediction of the Langmuir model and (b) Se(VI) on FeS: 1 g/L FeS, 1 and 10 mM of sulfate concentration, 24 h of contact time, pH 8.
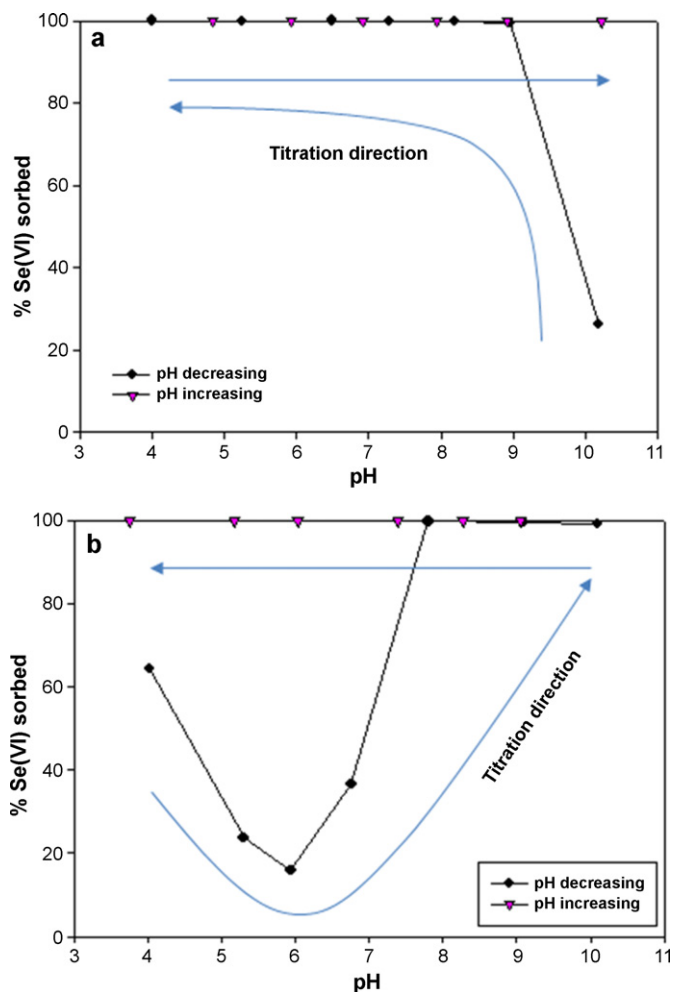
Fig. 4. Effect of pH on (a) removal of Se(IV) by FeS as pH was decreased from pH 10 and subsequently was increased and on (b) removal of Se(VI) as pH was increased from near pH 4 and subsequently was decreased: FeS = 1 g/L and Se(IV,VI) = 16.6 μM.
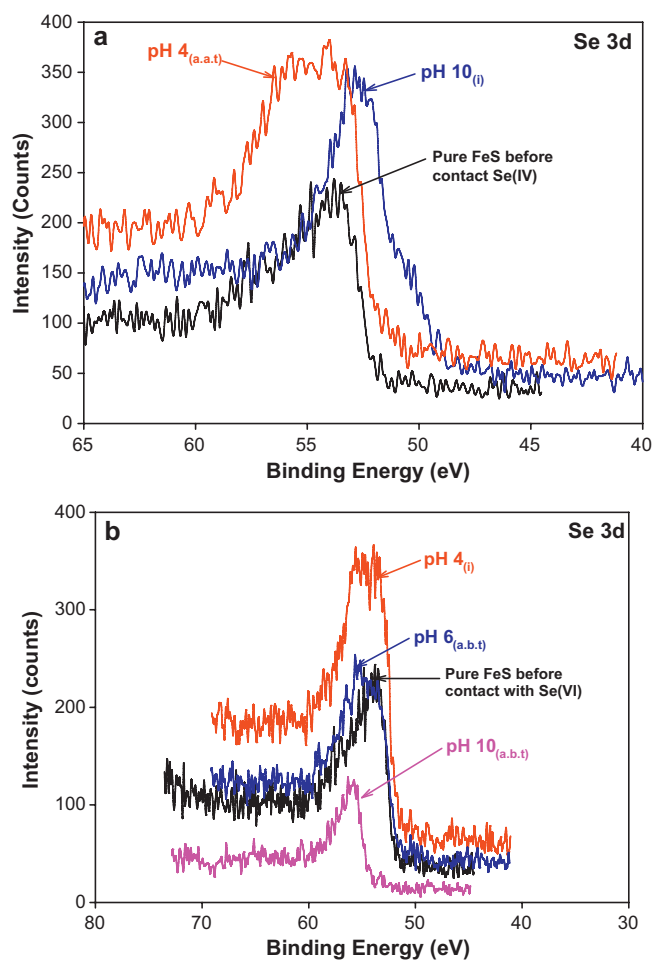

Fig. 5. High resolution Se 3d XPS spectra for FeS before and after contact with (a) Se(IV) (16.6 μM) at pH $10_{(i)}$ and pH $4_{(a.a.t)}$ and (b) Se(VI) (16.6 μM) at pH $4_{(i)}$, $6_{(a.b.t)}$, and $10_{(a.b.t)}$: FeS = 1 g/L, Se(IV,VI) = 16.6 μM, pH $6_{(a.b.t)}$ means solid sample obtained during the base titration.

not show the evidence of reduction of Se(IV) on the pH$_{(i)}$ sample, we cannot conclude that Se(IV) did not undergo reduction reaction because the XPS peak for Se(0) can be still overlapped by the Fe 3p spectra. In addition, no observation of red Se(0), as pH was initially adjusted to pH 10, could be due to low concentration ratio of Se(IV) to mackinawite, so that the red color could be screened by dark color.

Fig. 5b shows the Se 3d XPS spectra for FeS before and after contact with Se(VI). The pH $10_{(a.b.t)}$ sample shows shift of the main peak to higher binding energy, compared to FeS that had not contacted Se(VI). This indicates that Se(VI) could be reduced to forms such as Se(IV), Se(0), or Se(−II) by reaction with the FeS surface, but it is not assured because there is no report in literature presenting reduction of Se(VI) by iron sulfides. Moreover, this behavior is in contrast to what was observed for mixtures of Se(IV) and FeS at pH $4_{(i)}$, although comparable high removals are observed. However, it was known that the anion in GR interlayer can exchange with Se(VI) or that GR can co-precipitate with Se(VI) at high pH, followed by further reduction of Se(VI) [35]. These more reduced species on the FeS or the interlayer-trapped Se(VI) in GR may be more tightly bound to the surface or may form insoluble solid phases distinct from FeS. Such transformations would explain the behavior observed in the sorption envelope experiments. Unlike the pH $10_{(a.b.t)}$ sample, the Se 3d spectra of pH $4_{(i)}$ and $6_{(a.b.t)}$ samples looks similar to that of pure FeS, which indicates that there was negligible reduction of Se(VI).

4. Conclusions

Removal of Se(IV) by mackinawite was more rapid than Se(VI), but additional removal of Se(VI) was observed at longer contact time. Evidence for surface reactions of Se(IV) and Se(VI) on mackinawite was visible in removal pattern at pH 7 and pH 8, because they followed the pattern of a BET model for Se(IV) and Freundlich model for Se(VI). Sulfate had a negligible effect on removal of selenium by mackinawite, except the case at intermediate concentration of Se(VI) where sulfate improved removal, so it should not hinder application of the process to ash or scrubber pond water. Sorption hysteresis for Se(IV) and Se(VI) were observed, indicating that stable mixtures were formed.

Acknowledgements

Appendix A. Supplementary data

Supplementary data associated with this article can be found, in the online version, at doi:10.1016/j.jhazmat.2010.11.017.

References

[1] P.C. Zhang, D.L. Sparks, Kinetics of selenate and selenite adsorption desorption at the goethite water interface, Environ. Sci. Technol. 24 (1990) 1848–1856.

[2] P. Refait, L. Simon, J.M.R. Genin, Reduction of SeO_4^{2-} anions and anoxic formation of iron(II)–iron(III) hydroxy selenate green rust, Environ. Sci. Technol. 34 (2000) 819–825.

[3] S. Hyun, P.E. Burns, I. Murarka, L.S. Lee, Selenium(IV) and (VI) sorption by soils surrounding fly ash management facilities, Vadose Zone J. 5 (2006) 1110–1118.

[4] USEPA, Draft Aquatic Life Water Quality Criteria for Selenium, USEPA, Washington, DC, 2004 (USEPA Report. 822-D-04-001).

[5] I. Bodek, Environmental Inorganic Chemistry: Properties, Processes and Estimation Methods, Pergamon Press, New York, 1988.

[6] D. Peak, U.K. Saha, P.M. Huang, Selenite adsorption mechanisms on pure and coated montmorillonite: an EXAFS and XANES spectroscopic study, Soil Sci. Soc. Am. J. 70 (2006) 192–203.

[7] S.D. Faust, O.M. Aly, Chemistry of Water Treatment, 2nd ed., Ann Arbor Press, Chelsea, MI, 1998.

[8] E.T. Thompsoneagle, W.T. Frankenberger, U. Karlson, Volatilization of selenium by *Alternaria-Alternata*, Appl. Environ. Microbiol. 55 (1989) 1406–1413.

[9] J. Chung, R. Nerenberg, B.E. Rittmann, Bioreduction of selenate using a hydrogen-based membrane biofilm reactor, Environ. Sci. Technol. 40 (2006) 1664–1671.

[10] L.S. Balistrieri, T.T. Chao, Adsorption of selenium by amorphous iron oxyhydroxide and manganese-dioxide, Geochim. Cosmochim. Acta 54 (1990) 739–751.

[11] M. Duc, G. Lefevre, M. Fedoroff, Sorption of selenite ions on hematite, J. Colloid Interface Sci. 298 (2006) 556–563.

[12] Y.W. You, G.F. Vance, H.T. Zhao, Selenium adsorption on Mg–Al and Zn–Al layered double hydroxides, Appl. Clay Sci. 20 (2001) 13–25.

[13] C.H. Wu, S.L. Lo, C.F. Lin, C.Y. Kuo, Modeling competitive adsorption of molybdate, sulfate, and selenate on gamma-Al_2O_3 by the triple-layer model, J. Colloid Interface Sci. 233 (2001) 259–264.

[14] N. Zhang, L.S. Lin, D.C. Gang, Adsorptive selenite removal from water using iron-coated GAC adsorbents, Water Res. 42 (2008) 3809–3816.

[15] M.A. Elrashidi, D.C. Adriano, S.M. Workman, W.L. Lindsay, Chemical equilibria of selenium in soils – a theoretical development, Soil Sci. 144 (1987) 141–152.

[16] A.C. Scheinost, R. Kirsch, D. Banerjee, A. Fernandez-Martinez, H. Zaenker, H. Funke, L. Charlet, X-ray absorption and photoelectron spectroscopy investigation of selenite reduction by Fe(II)-bearing minerals, J. Contam. Hydrol. 102 (2008) 228–245.

[17] C. Bruggeman, A. Maes, J. Vancluysen, P. Vandenmussele, Selenite reduction in Boom clay: effect of FeS_2, clay minerals and dissolved organic matter, Environ. Pollut. 137 (2005) 209–221.

[18] A.C. Scheinost, L. Charlet, Selenite reduction by mackinawite, magnetite and siderite: XAS characterization of nanosized redox products, Environ. Sci. Technol. 42 (2008) 1984–1989.

[19] B. Batchelor, D.S. Han, E.J. Kim, Final Report: Novel Adsorbent-Reactants for Treatment of Ash and Scrubber Pond Effluents, US Department of Energy (DOE), National Energy Technology Laboratory (NETL), 2010 (DF-FG26-06NT42731).

[20] H.Y. Jeong, K.F. Hayes, Impact of transition metals on reductive dechlorination rate of hexachloroethane by mackinawite, Environ. Sci. Technol. 37 (2003) 4650–4655.

[21] E.C. Butler, K.F. Hayes, Kinetics of the transformation of trichloroethylene and tetrachloroethylene by iron sulfide, Environ. Sci. Technol. 33 (1999) 2021–2027.

[22] M. Wolthers, S.J. Van der Gaast, D. Rickard, The structure of disordered mackinawite, Am. Mineral. 88 (2003) 2007–2015.

[23] H.Y. Jeong, J.H. Lee, K.F. Hayes, Characterization of synthetic nanocrystalline mackinawite: crystal structure, particle size, and specific surface area, Geochim. Cosmochim. Acta 72 (2008) 493–505.

[24] D.S. Han, Sorption of arsenic, mercury, selenium onto nanostructured adsorbent media and stabilization via surface reactions, Ph.D. Dissertation, Zachry Department of Civil Engineering, Texas A&M University, College Station, TX, 2009, p. 403.

[25] B.C. Bostick, S. Fendorf, Arsenite sorption on troilite (FeS) and pyrite (FeS_2), Geochim. Cosmochim. Acta 67 (2003) 909–921.

[26] F. Demoisson, M. Mullet, B. Humbert, Investigation of pyrite oxidation by hexavalent chromium: solution species and surface chemistry, J. Colloid Interface Sci. 316 (2007) 531–540.

[27] E. Breynaert, C. Bruggeman, A. Maes, XANES–EXAFS analysis of Se solid-phase reaction products formed upon contacting Se(IV) with FeS_2 and FeS, Environ. Sci. Technol. 42 (2008) 3595–3601.

[28] W.H. Kuan, S.L. Lo, M.K. Wang, C.F. Lin, Removal of Se(IV) and Se(VI) from water by aluminum-oxide-coated sand, Water Res. 32 (1998) 915–923.

[29] S.L. Lo, T.Y. Chen, Adsorption of Se(IV) and Se(VI) on an iron-coated sand from water, Chemosphere 35 (1997) 919–930.

[30] M. Rovira, J. Gimenez, M. Martinez, X. Martinez-Llado, J. de Pablo, V. Marti, L. Duro, Sorption of selenium(IV) and selenium(VI) onto natural iron oxides: goethite and hematite, J. Hazard. Mater. 150 (2008) 279–284.

[31] A. Naveau, F. Monteil-Rivera, E. Guillon, J. Dumonceau, Interactions of aqueous selenium(−II) and (IV) with metallic sulfide surfaces, Environ. Sci. Technol. 41 (2007) 5376–5382.

[32] B.C. Bostick, S. Fendorf, B.A. Manning, Arsenite adsorption on galena (PbS) and sphalerite (ZnS), Geochim. Cosmochim. Acta 67 (2003) 895–907.

[33] E.J. Kim, B. Batchelor, Macroscopic and X-ray photoelectron spectroscopic investigation of interactions of arsenic with synthesized pyrite, Environ. Sci. Technol. 43 (2009) 2899–2904.

[34] D. Peak, D.L. Sparks, Mechanisms of selenate adsorption on iron oxides and hydroxides, Environ. Sci. Technol. 36 (2002) 1460–1466.

[35] S.C.B. Myneni, T.K. Tokunaga, G.E. Brown, Abiotic selenium redox transformations in the presence of Fe(II,III) oxides, Science 278 (1997) 1106–1109.

[36] B.C. Bostick, S. Fendorf, G.R. Helz, Differential adsorption of molybdate and tetrathiomolybdate on pyrite (FeS_2), Environ. Sci. Technol. 37 (2003) 285–291.

[37] D. Banerjee, H.W. Nesbitt, XPS study of reductive dissolution of birnessite by H_2SeO_3 with constraints on reaction mechanism, Am. Mineral. 85 (2000) 817–825.

[38] X. Liu, M. Fattahi, G. Montavon, B. Grambow, Selenide retention onto pyrite under reducing conditions, Radiochim. Acta 96 (2008) 473–479.